

PAPER • OPEN ACCESS

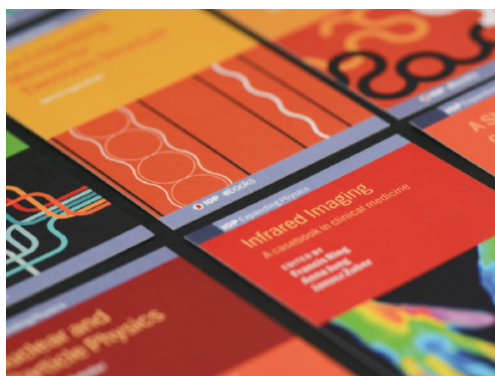
Effects of Force Fields on Interface Dynamics, in view of Two-Phase Heat Transfer Enhancement and Phase Management for Space Applications

To cite this article: P Di Marco and G Saccone 2017 *J. Phys.: Conf. Ser.* **923** 012019

View the [article online](#) for updates and enhancements.

Related content

- [Approaching to Gravity?](#)
Sebahattin Tüzemen
- [The interface dynamics of bicontinuous phase separating structure in a polymer blend](#)
Haruko Saito, Masahiro Yoshinaga, Takaaki Mihara et al.
- [Geometrical model of a self-propelled broken interface](#)
Miki Y Matsuo and Masaki Sano



IOP | ebooks™

Bringing together innovative digital publishing with leading authors from the global scientific community.

Start exploring the collection—download the first chapter of every title for free.

Effects of Force Fields on Interface Dynamics, in view of Two-Phase Heat Transfer Enhancement and Phase Management for Space Applications

P Di Marco, G Saccone

DESTEC, University of Pisa, Pisa, Italia

E-mail: p.dimarco@ing.unipi.it

Abstract. On earth, gravity barely influences the dynamics of interfaces. For what concerns bubbles, buoyancy governs the dynamics of boiling mechanism and thus affects boiling heat transfer capacity. While, for droplets, the coupled effects of wettability and gravity affects interface exchanges. In space, in the lack of gravity, rules are changed and new phenomena come into play. The present work is aimed to study the effects of electric field on the shape and behaviour of bubbles and droplets in order to understand how to handle microgravity applications; in particular, the replacement of gravity with electric field and their coupled effects are evaluated. The experiments spread over different setups, gravity conditions, working fluids, interface conditions. Droplets and bubbles have been analysed with and without electric field, with and without (adiabatic) heat and mass transfer across the interface. Furthermore, the results of the 4 ESA Parabolic Flight Campaigns (PFC 58, 60, 64 & 66), for adiabatic bubbles, adiabatic droplets and evaporating droplets, will be summarized, discussed, and compared with the ground tests.

1. State of the art

Boiling and evaporation are ubiquitous phenomena. They are relevant for all the industrial applications involving heat transfer mechanisms, most of all: electrical power production. In both phenomena, gravity has a relevant role: it is responsible of bubble detachment during boiling [1], [2] and “flattens” the droplets [3] assisting heat transfer in both processes. The present study wants to extend and use these mechanisms, which are the most efficient heat transfer methods, to space applications. Phase separation and thermal management of space stations and satellites are becoming of growing interest and the reduction of size and weights calls the increase of systems performances and efficiencies [4].

The lack of gravity in such applications can be balanced by the use of a tunable electric field (EF), which creates body forces that substitute gravity. Many published works are available in literature proving the viability of this solution for microgravity applications [5][6][7][8][9][10][11][12].

1.1. Boiling

Boiling heat transfer has been widely studied in the past, in particular, several studies have addressed and speculated on the mechanisms leading to critical heat flux (CHF), the limiting condition of all boiling heat transfer processes, generally associated with the formation of an irreversible dry spot responsible of a drastic reduction of the local heat transfer coefficient, which can lead to catastrophic burnout of the boiling surface. Rosenhow [2] and Zuber [1] are two of the milestones in



the explanation of boiling mechanics and limits. In the present study we want to underline the importance of the electric field in increasing the limiting value of CHF, thus increasing safety and capacity of the heat transferred from a surface.

By considering the formation of vapor jets, their velocity and the competition between vapor, moving upwards, and liquid, moving downwards, Zuber [1] proposed a correlation ($K = 0.131$):

$$q''_{CHF} = Kh_{lv}\rho_v \left[\frac{g\sigma(\rho_l - \rho_v)}{\rho_v^2} \right]^{0.25} \quad 1$$

Nowadays several techniques can be adopted to enhance CHF beyond the limits predicted by these correlations. Specifically, CHF can be enhanced using passive or active techniques, such as micro-structured surfaces and electric field, respectively.

It is well established that in CHF the dynamics of the contact line plays an important role, and surface conditions, e.g. roughness, wettability and porosity play a role too. As we mentioned, buoyancy determines the efficiency of the boiling process creating bubbles detaching forces; however, it has been shown that the application of an external electric field can improve the boiling heat transfer performance increasing bubble detaching forces and modifying the wettability of the fluid-surface system [13] [14][15][16][17].

1.2. Drop evaporation

When a sessile droplet is exposed to a static electric field, its shape is defined by a balance between surface tension, electrostatic and gravitational forces. The surface tension component tends to make the droplet spherical, the electrostatic force elongates the droplet towards the electrode and the gravitational "flattens" the droplet. The droplet shape and its evaporation rate are strictly linked to triple line movement and wettability. Force fields (namely, a static electric field and the gravitational one) do have a role on triple line dynamics, wettability and heat transfer [18]. Studies showed that different modes of evaporation are possible, depending on the triple line dynamics [19][20][21][22] and thus depending on the hysteresis of the contact angle [23]. A drop can evaporate with a constant contact area overtime, the triple line is pinned and the evaporation is characterized by a decrease of the contact angle during the evaporation. A drop can also evaporate with a constant contact angle overtime; in this case evaporation occurs with a recession of the triple line [24].

2. Interface stability under the action of the electric field

One important first step in deriving an expression for the volumetric electric force (f_e''') that acts on a fluid has been proposed by Landau and Lifshitz [25]:

$$f_e''' = \rho_f E - \frac{\epsilon_0 E^2}{2} \nabla \epsilon_R + \frac{\epsilon_0}{2} \nabla \left(\rho \left(\frac{\partial \epsilon_R}{\partial \rho} \right)_T E^2 \right) \quad 2$$

Only the first term (electrophoresis) depends on the sign of the electric field, but it is present only when free charge (ρ_f) buildup occurs. It doesn't play a role in the present study, where dielectric fluids are involved. The second and third terms are termed dielectrophoresis and electrostriction. The former one depends on the gradient of the dielectric constant (ϵ_R , which may occur either from thermal gradients and/or from phase discontinuities) and the latter one is due to the gradient of E^2 . According to continuum mechanics, Eq.2 can be expressed as the divergence of a stress tensor. $\bar{\bar{T}}_e$ is the Maxwell stress tensor, that is:

$$f_e''' = \nabla \bar{\bar{T}}_e \quad 3$$

The resulting force acting on a surface S (\bar{n} , its unit vector) is:

$$F_e = \iint_S \bar{\bar{T}}_e \cdot \bar{n} dS \quad 4$$

Thus, the momentum balance on a bubble in the direction perpendicular to the surface can be written as

$$F_\sigma + F_b + F_p + F_e = 0$$

5

where the different terms are defined as:

Forces	Bubbles	Droplets	
Surface Tension	$F_\sigma = -\pi D \sigma \sin \theta$	$F_\sigma = -\pi D \sigma \sin \theta$	6
Buoyancy	$F_b = (\rho_f - \rho_g) g V$	$F_b = (\rho_g - \rho_f) g V$	7
Pressure	$F_p = \frac{\pi D^2}{4} \left(\frac{2\sigma}{R_0} - \rho_f g H \right)$	$F_p = \frac{\pi D^2}{4} \left(\frac{2\sigma}{R_0} + \rho_f g H \right)$	8
Electrical	$F_e = \int_S \overline{T_{e,g}} \cdot \vec{n} dS$	$F_e = \int_S \overline{T_{e,g}} \cdot \vec{n} dS$	9

Table 1: Force balance of Eq. 5 extended for both bubbles and droplets

Difficulties in calculating the Maxwell stress tensor arise from the evaluation of the local electric field, which is affected by bubble/droplet size and shape and, in turn, it influences bubble/droplet size and shape. Clearly, the term E^2 and its gradient are the dominating terms in the Maxwell stress tensor which determines the forces associated with the electric field.

The application of an external electric field, results in an increase in pressure and surface tension, obtained respectively by an increase in the height of the shape, a higher curvature radius at its top and a larger contact angle. This behavior has been experienced in all cases: bubble or droplet, micro or normal gravity. The electric field always “calls” the object towards the direction of higher potential (see Figure 1, 2, 3, 4).

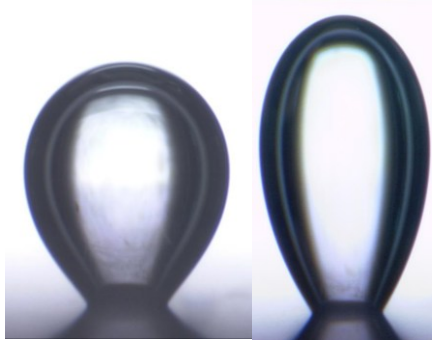


Figure 1: bubble with and without EF (3.33 MV/m) normal gravity field

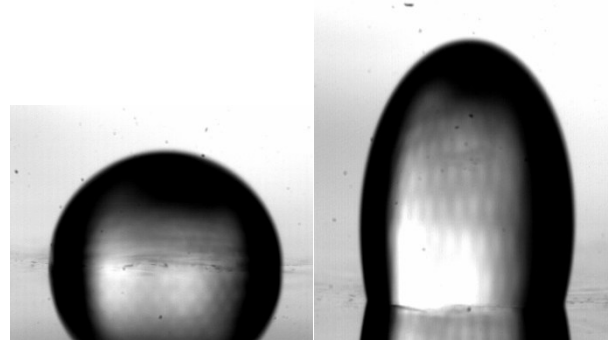


Figure 2: droplet with and without EF (1.25 MV/m) normal gravity field

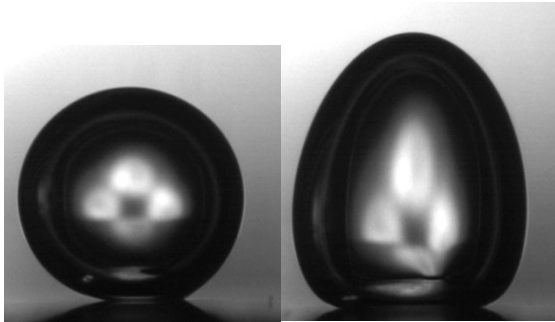


Figure 3: bubble with and without EF (3.33 MV/m)
microgravity (58th PFC 2013 – 60th PFC 2014)

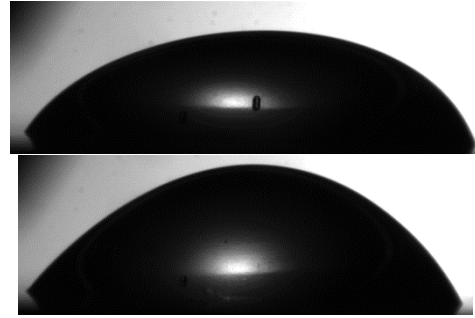


Figure 4: droplet with and without EF (0.833MV/m)
microgravity (64th PFC 2016 – 66th PFC 2017)

A last use of mathematics is here necessary to evaluate the force balance in the radial direction. This force balance has been proposed initially for droplets [26], but found its use also to understand bubble behavior. Considering a slice of a resting droplet (see Figure 5) as control volume, a balance between pressure and surface tension is achieved. Forces are shown with arrows.

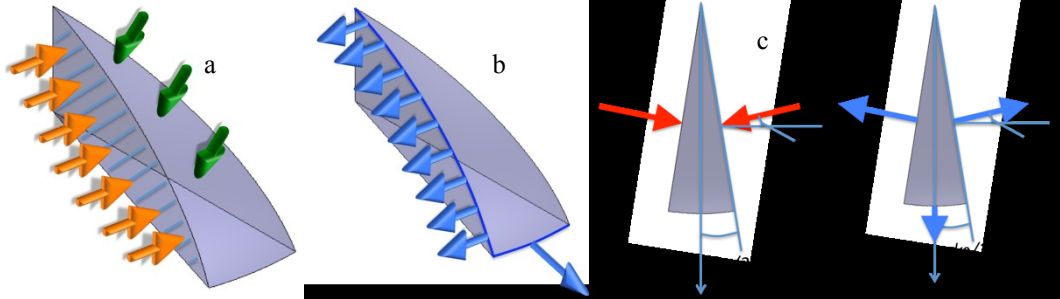


Figure 5: Slice of a droplet. Pressure of the liquid in orange. Pressure of air in green. Surface tension in blue.

The pressure, and therefore, spreading driving force can be written as:

$$F_p = 2 \iint \left(p_f(z) - p_g(z) \right) (\vec{n} \cdot \vec{r}) dr dz = \int_0^H \int_0^{r(z)} \left(p_f(z) - p_g(z) \right) d\phi dr dz \quad 10$$

The surface tension, and therefore, restraining force can be written as:

$$F_\sigma = 2 \sigma L \sin\left(\frac{d\phi}{2}\right) + \sigma \cos\vartheta r d\phi = \sigma L d\phi + \sigma \cos\vartheta r d\phi \quad 11$$

Finally, the equilibrium of the slice $d\phi$ is:

$$\int_0^H \int_0^{r(z)} \left(p_f(z) - p_g(z) \right) dr dz = \sigma L + \sigma r \cos\vartheta \quad 12$$

or:

$$F_p = F_\sigma \quad 13$$

Integration of the first term of this balance has to be carried on numerically, point by point. In this study it has been performed from the top to the base. It is worth noting that in the restraining force (Eq. 11) the second term can be either positive or negative (see the direction of blue arrows in Figure 5d), depending on the value of the contact angle. Again, in presence of electric field, we will derive the resulting electric force from the algebraic sum of the others.

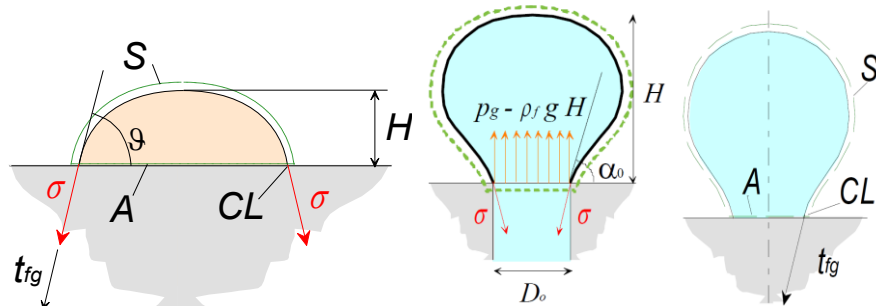


Figure 6: Control volume for force balances showing the direction of the parameters

3. Experimental apparatus

Due to the nature of the experiments, different experimental setups will be here described.

3.1. Bubbles setup

For what concerns bubbles (see Figure 7), it consists in a bubble generator, comprising a flat stainless steel plate with a circular orifice of 0.5 mm internal diameter drilled on it. The orifice was fed with nitrogen by means of a gas flowrate controller. In this way, continuous trains of detaching bubbles, or individual bubbles growing very slowly can be generated. The test cell is an aluminum box filled with the test liquid (FC-72). An electric potential up to 25 kV dc could be applied to a washer-shaped electrode (10x4 mm, 1 mm thickness), located 6 mm above the plate and centered with the orifice axis.

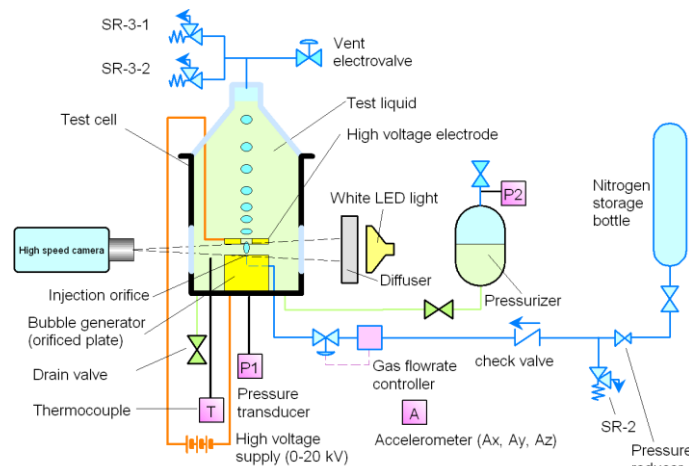


Figure 7: Experimental setup for bubbles (58th PFC 2013 – 60th PFC 2014)

3.2. Droplet setup

For droplets instead (see Figure 8), the experiment's configuration consists of the same test cell provided with a stainless steel plate surmounted by a washer shaped electrode, 6 mm far from the surface, connected with a power supply generating up to 7.5 kV. A syringe connected to a micrometric slide, moved by a stepper motor, assures constant volumetric flow rate through an orifice drilled on the plate. Different working fluids have been tested (Water, FC72, HFE7100).

3.3. Data processing

Images are acquired with a high-resolution camera, equipped with microscopic lens, at 500 fps for bubbles and 50 fps for droplets. The definition achieved was about 5 $\mu\text{m}/\text{pixel}$.

The profile and all relevant parameters are derived via a dedicated software implemented in MATLAB, with the aid of the Image processing toolbox. At first, the background is subtracted to reduce noise, the contour is identified with a threshold (Canny method) and the contact angle is

measured by polynomial regression of the points of the profile close to the contact line. The number of pixel of the regression curve used is function of the height of the drop, while the degree of the polynomial curve is 2 and all points are weighted in function of the distance from the contact point.

The radius of curvature at drop top also is calculated fitting the 7 highest points of the profile with a parabola, while the drop volume is calculated with Guldin theorem, specific for rotational bodies. So on, all geometrical parameters of interest are derived from the image processing code.

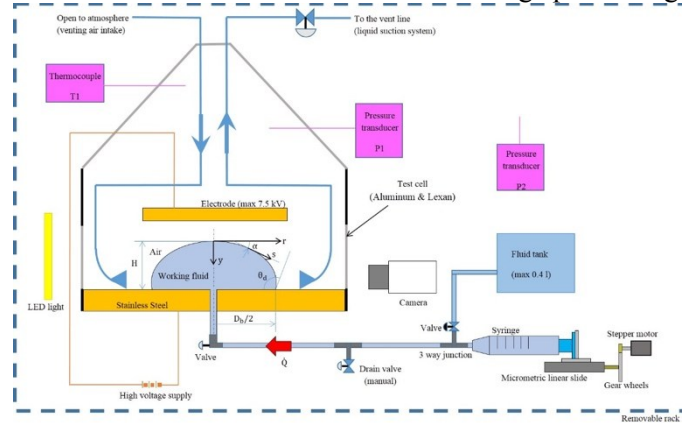


Figure 8: experimental setup for droplets (64th PFC 2016)

4. Results and discussion

A complete review of all the results is behind the purpose of this work. In the present paper we would like to summarize all the findings showing common aspects, achieved goals and particular experienced behaviors. In general, this work can confirm that:

- The electric field exerts a negative radial force (see Figure 10, Figure 12). It means that it shrinks bubbles and droplets. This force is responsible of:
 1. elongation in the vertical direction (see Figure 1, 2, 3, 4),
 2. bubble departure with reduced diameter in microgravity (see Figure 13),
 3. when dielectric fluids are used, formation of a liquid jet; when water is used, dielectric breakup (see Figure 15 and 16).
- The electric field exerts a negative vertical force. It means that pushes bubbles and droplets against the surface (Figure 9, Figure 11).

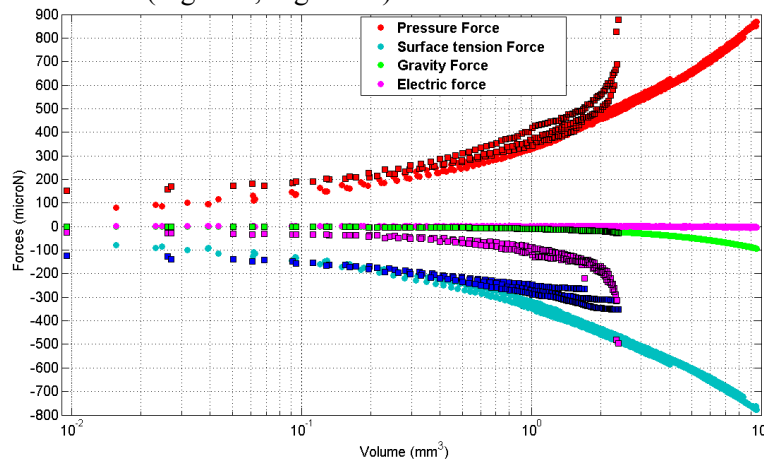


Figure 9: Vertical force balance for the 0 kV (circles) and 7.5 kV (squares with black border) cases. Droplet normal gravity.

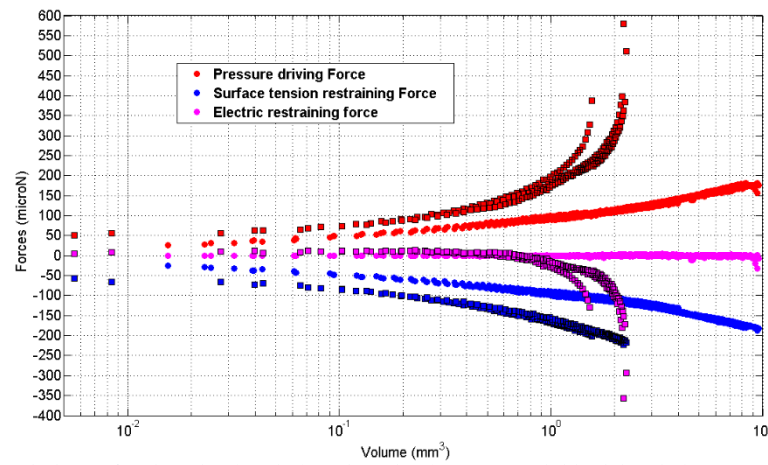


Figure 10: Radial force balance for the 0 kV (circles) and 7.5 kV (squares with black border) cases. Droplet normal gravity.

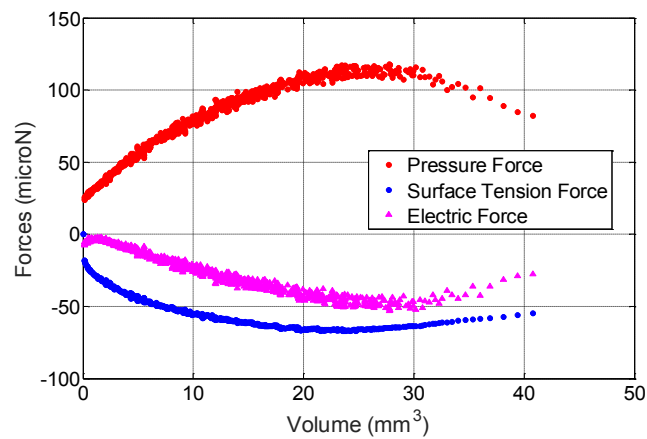


Figure 11: Vertical force balance. Bubbles in microgravity, EF applied

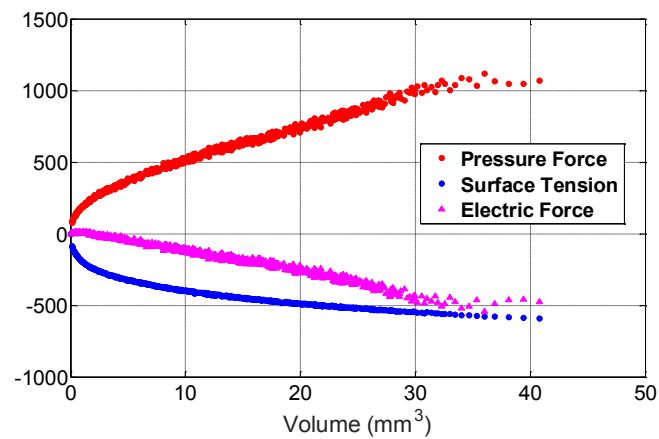


Figure 12: Radial force balance. Bubbles in microgravity, EF applied

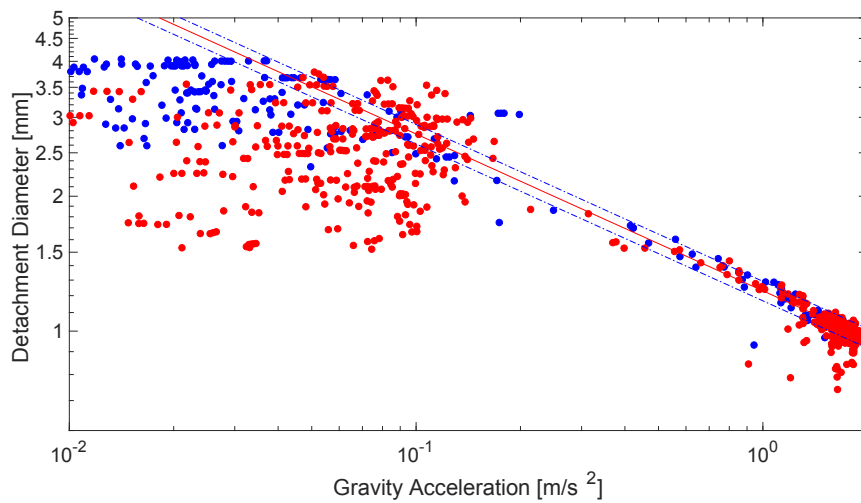


Figure 13: Detachment diameter vs gravity with (red dots) and without (blue dots) electric field.

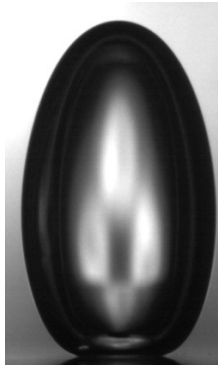


Figure 14: bubble in microgravity, right before departure

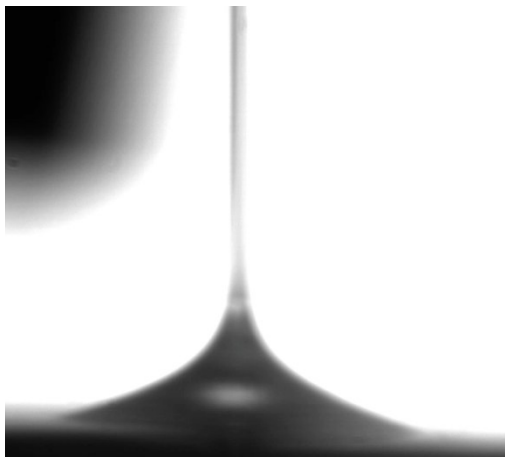


Figure 15: Taylor cone in microgravity and liquid jet, HFE7100

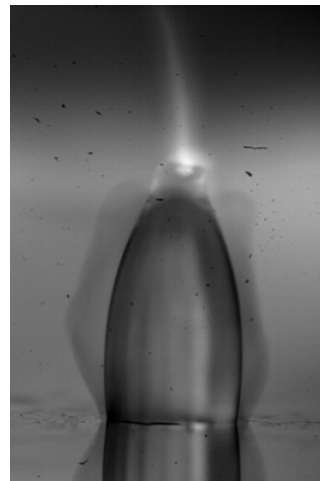


Figure 16: Dielectric breakup, Water

5. Heat and mass transfers with electric field

Introducing Eq. 2, we affirmed that the electric force is a volume force. Thus, the resulting electric force depends on the volume. By analyzing a droplet withdrawal, we found some relevance for what concerns droplet evaporation assisted by electric field. Looking at Figure 17, we can verify that the

vertical electric force presses the droplet against the surface, but its effect vanishes with vanishing volume.

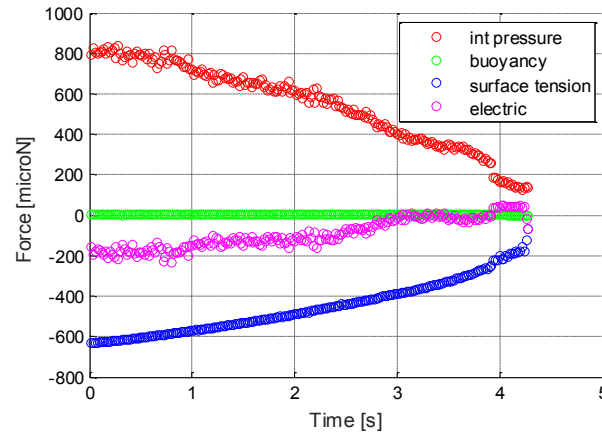


Figure 17: Vertical force balance, droplet withdrawal (reducing its volume with time), microgravity, with electric field

By only considering this fact, we should honestly say that we do not necessarily expect an increase in drop evaporation heat transfer; further studies are currently ongoing to better assess this. The enhancement of the heat transfer might also be induced by the flow of the “corona wind”, which is caused by the gas ionisation near the electrode [27][10].

For what concerns boiling, a study has been performed showing an increase of about 27% in CHF and heat transfer coefficient (HTC, see Figure 18 and Figure 19).

Here, again, when the EF is applied, an “electric wind” attracts the bubbles towards the centre of the electrode (direction of rising voltage). We can speculate that this electro-convection effect is responsible for the increase in HTC and CHF. Furthermore, it is worth noting that bubbles are shrunk with respect to the normal case (Figure 20). This is due to the electric field force, which, when it can distribute around the interface properly (undisturbed by other bubbles) creates the radial force that shrinks the bubbles. It is probably the case when the irreversible dry spot, coinciding with CHF, generates: it is smaller and the electric field always acts in order to reduce its size due to the action of radial forces.

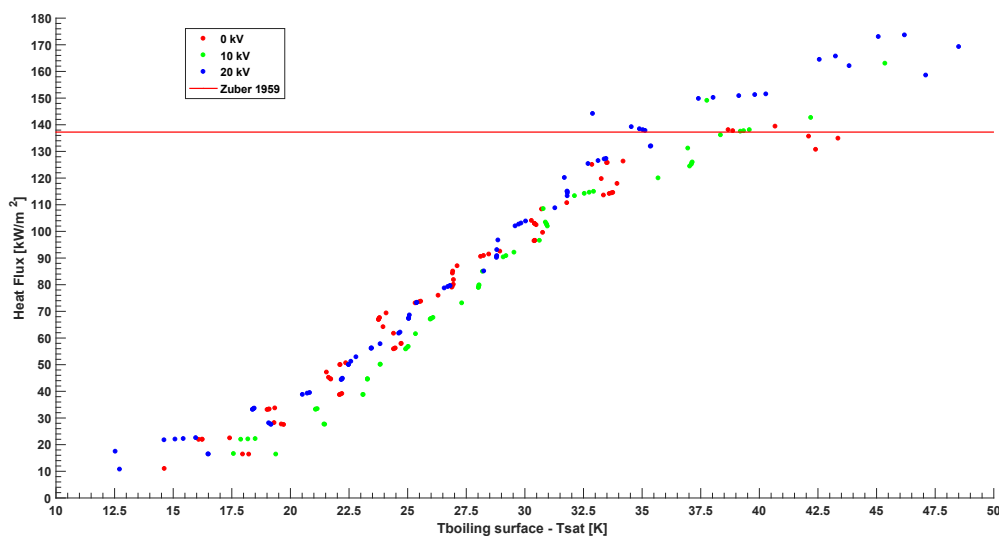


Figure 18: boiling curve of FC72 in pool boiling, with and without EF

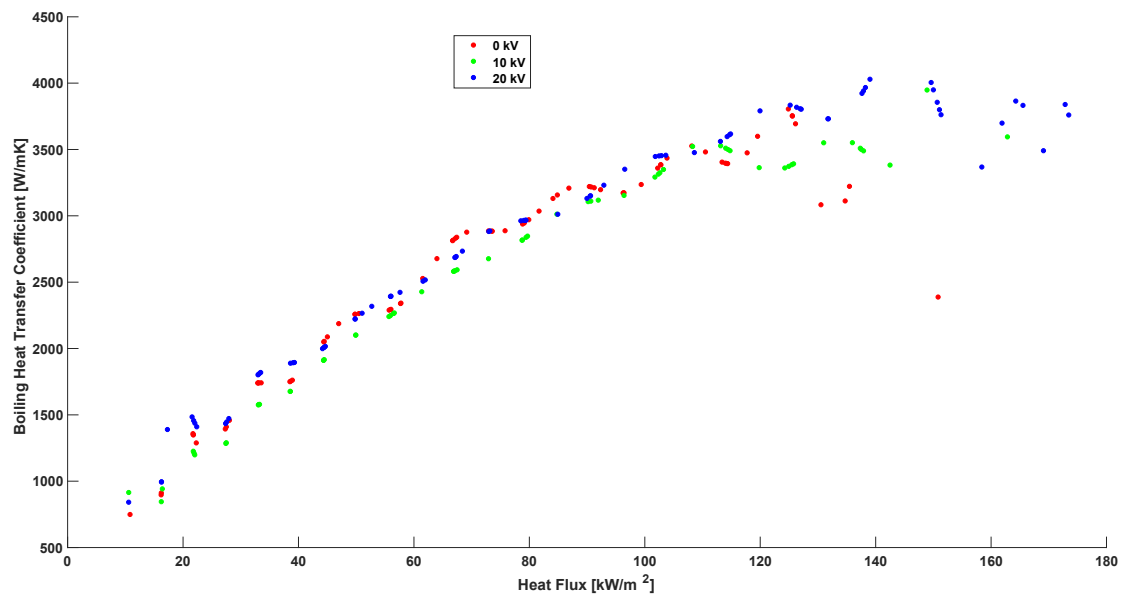


Figure 19: heat transfer coefficient (HTC) of FC72 in pool boiling, with and without EF

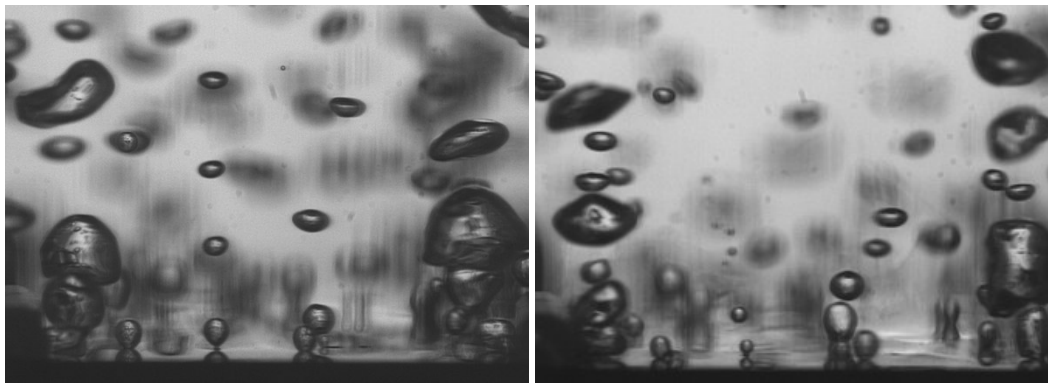


Figure 20: 0 and 20kV (3.33MV/m), 30kW/m²

In general, the electric field enhances boiling heat transfer coefficient for low heat fluxes (nucleate boiling region) and for high heat fluxes (close to CHF and at CHF). And the reason of CHF suppression when the electric field is applied is due to the force balances discussed previously. Figure 21 shows a recorded experiment performed at a heat flux close to CHF at 0kV, switching the EF on and off. We can affirm without any doubt that the electric field is quenching the dryspot and bringing back the surface to the fully developed nucleate boiling regime.

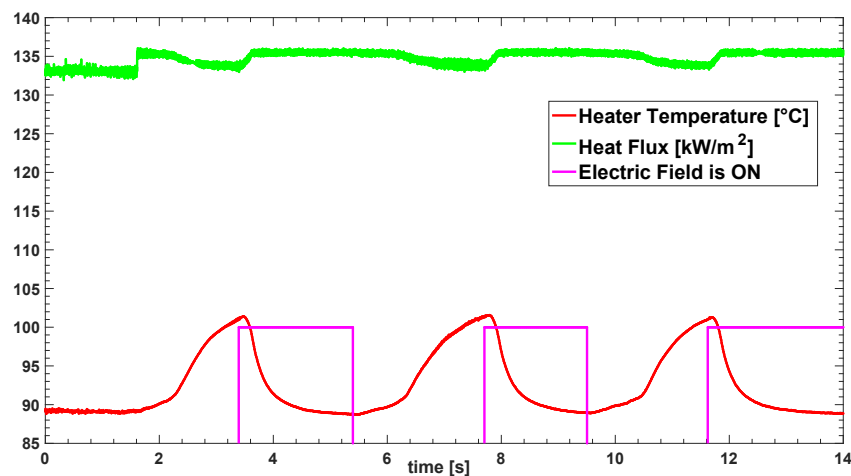


Figure 21: time history of CHF suppression induced by EF application

6. Conclusions

The effects of the electric field on interfaces (bubbles and droplets) have been evaluated. From the activity carried on at DESTEC, University of Pisa, we found that the electric field always acts by shrinking the interface. This can lead either to bubble departure, liquid jet or simply to a rise in the height of the interface.

For what concerns heat and mass transfer in droplets, even if the electric force is negligible, due to small volumes, the “corona wind” may assist in creating a strong flow of air, which can promote heat transfer and replace gravitational natural convection. The effect of electroconvection has been found of particular concern for bubbles during boiling experiments. In general, for bubbles, we have to mention that the EF provides a reliable and repeatable departure diameter also in microgravity.

In all cases the electric field normally concurs with gravity in assisting heat transfer, but it will be the main source of phase separation and management when gravity lacks.

References

- [1] Zuber N, 1959, Ph.D. thesis, Research Laboratory, Los Angeles and Ramo-Wooldridge Corporation, University of California, Los Angeles, CA
- [2] Rohsenow W. M., 1952, Transactions of ASME, Vol.74, pp. 969-976
- [3] Brutin D, Carle F, Academic Press, Oxford, 2015, Pages 383-393, ISBN 9780128007228, <https://doi.org/10.1016/B978-0-12-800722-8.00025-4>
- [4] Zhang H, Mudawar I, 2008 11th Intersociety Conference on Thermal and Thermomechanical Phenomena in Electronic Systems, Orlando, FL, 2008, pp. 949-959. doi: 10.1109/ITHERM.2008.4544370
- [5] Di Marco P, Grassi W, 1993, J. Enhanced heat transfer 1:99-114
- [6] Di Marco P, Grassi W, 1996, Proc. of Eurotherm Seminar 48. Eds. D. Gorenflo, D. Kenning, C. Marvillet, D. Paderborn, Pisa: ETS, 1:255-264
- [7] Di Marco P., Grassi W, 2007, Multiphase Sci. Technol. 19.2, pp. 141-165.
- [8] Di Marco P, Kurimoto R, Saccone G, Hayashi K, Tomiyama A, Experimental Thermal and Fluid Science, 2013, Vol.49, P.160, DOI: 10.1016/j.expthermflusci.2013.04.015.
- [9] Di Marco P, Kurimoto R, Saccone G, Hayashi K, Tomiyama A, 2014, 15th Int. Heat Transfer Conference, Kyoto, Japan, paper 8960, pp. 1-11.
- [10] Vancauwenberghe V, Di Marco P, Brutin D, Colloids and Surfaces A: Physicochemical and Engineering Aspects, Volume 432, 5 September 2013, Pages 50-56, ISSN 0927-7757, <https://doi.org/10.1016/j.colsurfa.2013.04.067>.
- [11] Gibbons MJ, Howe CM, Di Marco P, Robinson AJ, 2016, J. Phys.: Conf. Ser. 745 032066, 7th

- European Thermal-Sciences Conference (Eurotherm2016), doi:10.1088/1742-6596/745/3/032066
- [12] Di Marco P, Pedretti F, Saccone G, 2013 Transfer, Fluid Mechanics, and Thermodynamics. In: Eighth World Conference on Experimental Heat Transfer, June 16 20, 2013, Lisbon, Portugal.
 - [13] Sharifi P, 2011, PhD Thesis, Southern Illinois University at Carbondale, UMI Number: 3460461.
 - [14] Zaghdoudi MC, Lallemand M, 1997, Proc. Int. Symp. on the physics of heat transfer in boiling and condensation, Moscow, May 1997, pp. 335-340.
 - [15] Zaghdoudi MC, Lallemand M, 2005, Arabian Journal for Science and Eng. 30, 189–212.
 - [16] Bonjour E, Verdier J, Weil L, 1962, AIChE-ASME 5th Nat. Conference, Houston, USA
 - [17] Allen PHG, Karayiannis T 1995 Heat Recovery Systems & CHP, 5 pp. 389-423
 - [18] Saccone G, Kurimoto R, Bucci M, Di Marco P, Tomiyama A, 2015, 7th European-Japanese Two-Phase Flow Group Meeting 12 pages
 - [19] Picknett RG, Bexon R, 1977, J. Colloid Interface Sci. 61 (2), 336 350.
 - [20] Bourge's-Monnier C, Shanahan MER, 1995, Langmuir 11 (7), 2820 2829.
 - [21] Shanahan MER, 2001a Langmuir 17, 3997 4002.
 - [22] Shanahan MER, 2001b Langmuir 17, 8229 8235.
 - [23] Kulinich SA, Farzaneh M, 2009, Appl. Surf. Sci. 255, 4056 4060.
 - [24] Brutin D, Sobac B, Academic Press, Oxford, 2015, Pages 25-30, ISBN 9780128007228, <https://doi.org/10.1016/B978-0-12-800722-8.00003-5>.
 - [25] Landau LD, Lifšitz EM, 2nd edn. Pergamon, New York (1984)
 - [26] Saccone G, 2014, Master Thesis, University of Pisa – CEA Saclay. <https://etd.adm.unipi.it/t/etd-05212014-193232/>
 - [27] Ahmedou SAO, Rouaud O, Food Bioprocess Technol. 2 (2009) 240–247.